ON THE VELOCITY PROFILE OF THE TURBULENT BOUNDARY LAYER ON ROTATING IMPELLER BLADINGS

By

E. LITVAI and L. PRESZLER

Department of Fluid Mechanics, Technical University, Budapest

(Received April 1, 1969)

Presented by Prof. Dr. J. GRUBER

1. Introduction

Some previous investigations made on a centrifugal impeller, 5 meter in diameter, by a withrotating observer [1] indicate that the development of the turbulent boundary layers in rotating systems may be quite different from that in non-rotating ones.

Because of the complex nature of the phenomenon, stepwise approximation of the problem seems to be the only possibility. At the beginning the velocity profiles at different points of the boundary layers on rotating blades were measured in order to compare them with the ordinary velocity profiles, and to detect the effect of the rotation on this degree.

The present paper describes the experimental apparatus, the instruments and the methods of investigation (Chapter 2). According to the experimental results detailed in Chapter 3, in spite of the considerable scatter, both the logarithmic "law of the wall" and the nearly sinusoidal "law of the wake", which represent the basic features of the turbulent boundary layers in stationary systems [2] may be taken as valid for rotating systems too, although in a somewhat different form. The deviation of the slope of the logarithmic profile could doubtless be observed.

Chapter 4 presents a simplified theory based on a hypothesis of the damping effect of the Coriolis forces [3] and on the concept of the mixing length. This theory gives the slope of the logarithmic profile for the case of rotation, in agreement with the measured values.

2. Test apparatus and experimental methods

The impeller (Figs. 1 and 2) consisting of a wooden lower disc (1), an upper disc (2) and 12 blades (3) made of aluminium sheet, with steel tube underframe (4) and 4 wheels, rotates on a concrete runway (5).

The air inlet (6), the grid (7) and the vanes (8) applied to assure a homogeneous velocity distribution in the impeller are suspended on the roof.

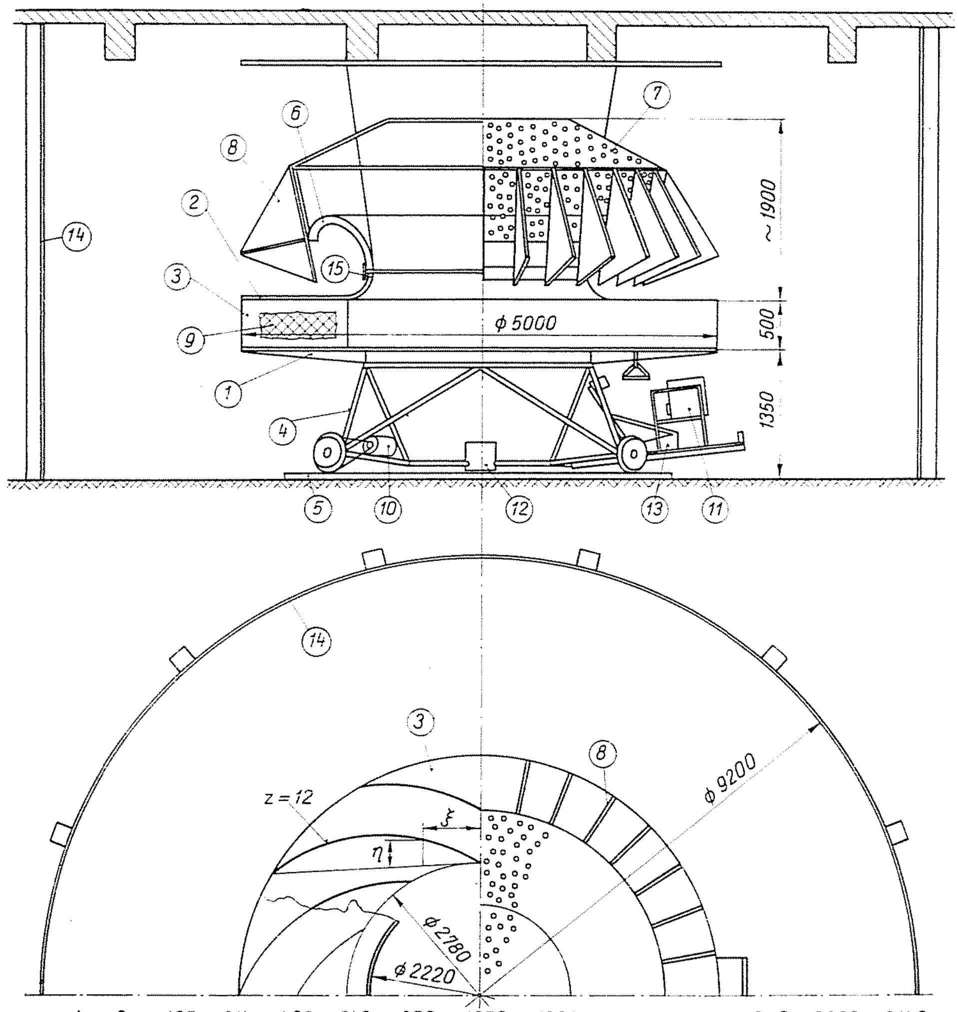

ξ	0	107	214	428	642	856	1070	1284	1498	1710	1926	2033	2140
η	0	45	110	230	310	360	368	348	290	210	110	52	0

Fig. 1. The test apparatus

The axial gap between the stationary and rotating parts of the gadget is covered by a strip of felt (15). This is important because in this way a two-dimensional boundary layer without remarkable secondary flows could be obtained in the vicinity of the half breadth of the blades [1], ((9) in (Fig. 1).

The power for the electromotor (10), for the anemometer (11) and for light was supplied by slip rings (12).

The observer is sitting on the seat (13) and carries out the measurements rotating with the impeller.

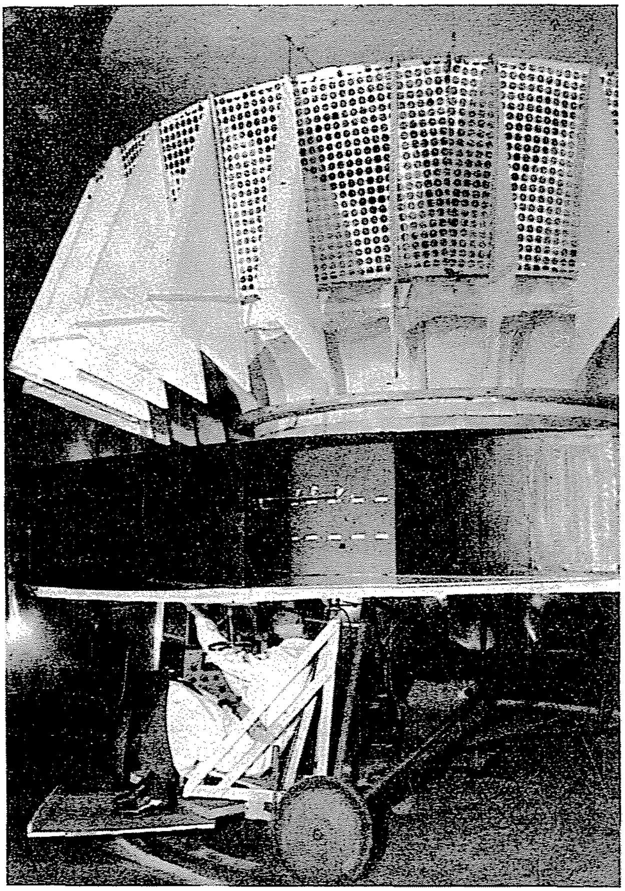

Fig. 2. General view of the gadget

The dimensions of the apparatus are shown in Fig. 1.

During the experiments reported below the maximum shaft speed was nearly $n = 18$ r. p. m. corresponding to a Reynolds number $Re = 1.7 \cdot 10^6$, calculated from the diameter of the impeller, from the peripheral velocity and from the kinematic viscosity of the air.

The loci of measurement are defined by the coordinate system shown in Fig. 3.

Two different basic cases must be distinguished, depending upon the side the measurements were carried out. Measurements on the pressure side (Fig. 3a) are marked by P, whereas the measurements on the suction side (Fig. 3b) by S.

Two further versions arose from the modification of the blade by a wooden streamline body according to B in Fig. 3a and 3b, respectively.

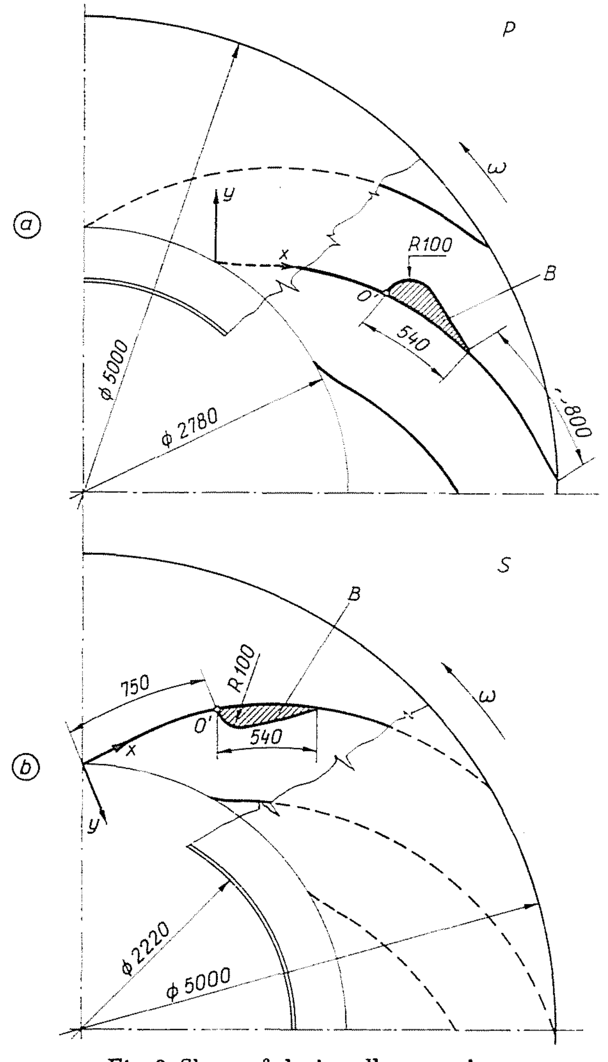

Fig. 3. Shape of the impeller, notations

Measurements made in the presence of the streamline body are marked by B.

The velocity measurements were made by means of a hot wire anemometer system DISA. The distance of the probe from the wall (y) could be varied during the rotation. The instrument shown in Fig. 4 permitted only measurements at fixed values of y, whereas the other one shown in Fig. 5, moved by a Bowden cable, could be stopped everywhere.

The slightest distance from the wall measured was 1 mm. The hot wire probe could not more approach the wall on account of the danger of breaking and of the vibrations.

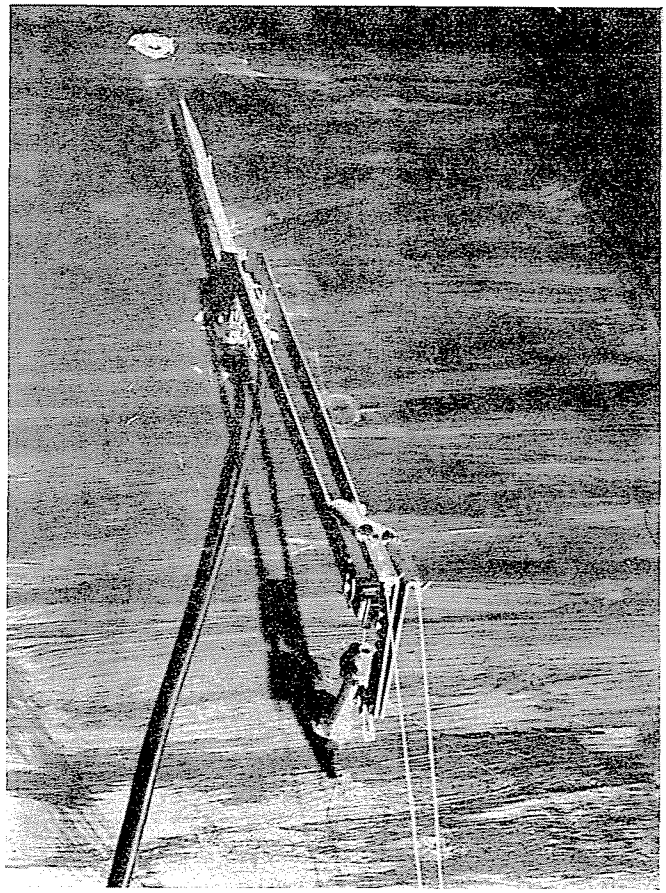

Fig. 4. Probe moved by a ratchet mechanism

Strong velocity fluctuations in the impeller caused by inhomogeneities not removed in the turning vane system ((6)—(8) in Fig. 1) produced an unavoidable series of errors. The accuracy of the measurements was considerably decreased by reading values fluctuating at a few Hz frequency.

The calibration of the hot wire probes took place at the periphery of the impeller at a distance of 50 mm over the upper disc ((2) in Fig. 1). The velocity in the surrounding air caused by the rotation of the impeller was taken into account by determining it in the stationary system.

3. Experimental results

About 30 velocity profiles have been measured, some of them are presented below.

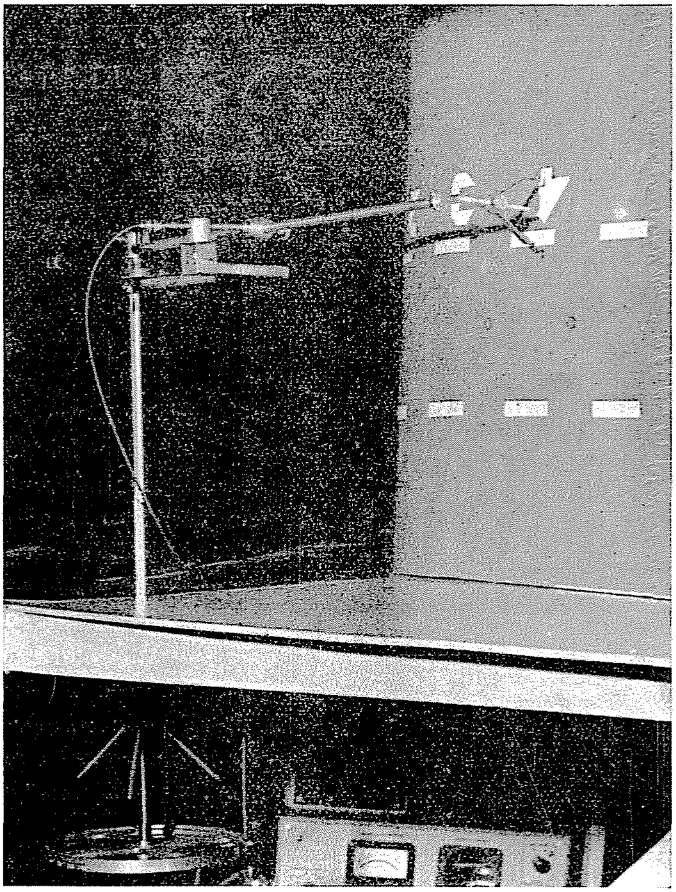

Fig. 5. Probe for measurements at arbitrary distances from the wall

For the further evaluation the knowledge of the frictional velocity defined by

$$u^* = \sqrt{\tau/\varrho} \tag{1}$$

was necessary.

Since the points of measurement reached hardly into the laminar sublayer, for a few values of y near the wall u^* has been calculated, making use of the formula

$$\frac{yu^*}{\nu} = \frac{w}{u^*} \tag{2}$$

valid in the laminar sublayer [4]. The values of u^* plotted as in Fig. 6 have then been extrapolated to $y = 0$. The estimated error of the procedure is at most ± 10 percent.

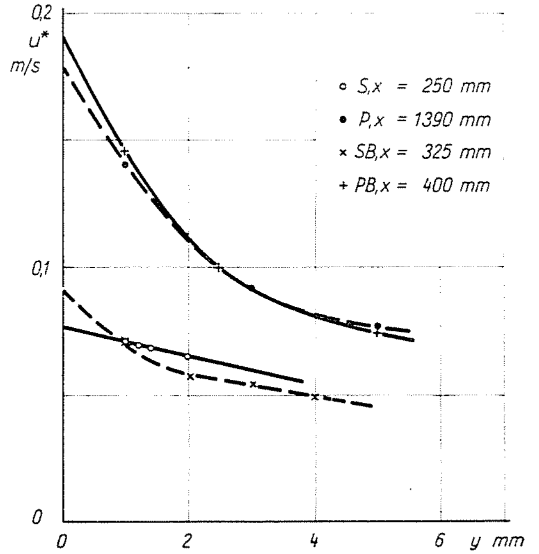

Fig. 6. Extrapolation of the frictional velocity

The velocity profiles are represented in semilogarithmic diagrams (Fig. 7a—f) as relationships between the dimensionless quantities

$$w^* = w/u^* \tag{3}$$

and

$$y^* = \frac{yu^*}{\nu} . \tag{4}$$

Figs 7a and 7b show profiles measured at the suction side whereas 7c and 7d show measured ones at the pressure side of the blading in the absence of the streamline body (B in Fig. 3).

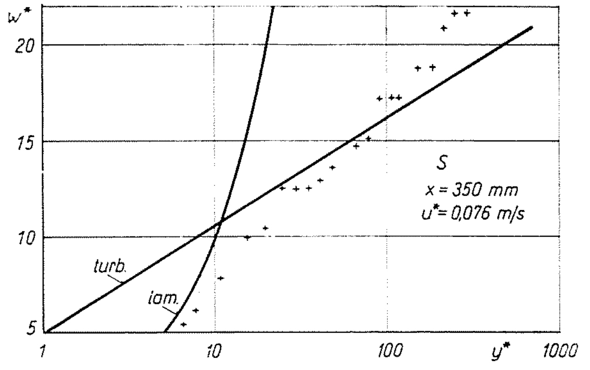

Fig. 7a—f. Dimensionless velocity profiles

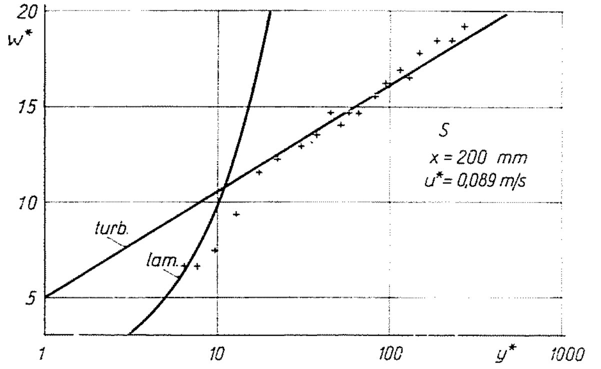

Fig. 7b

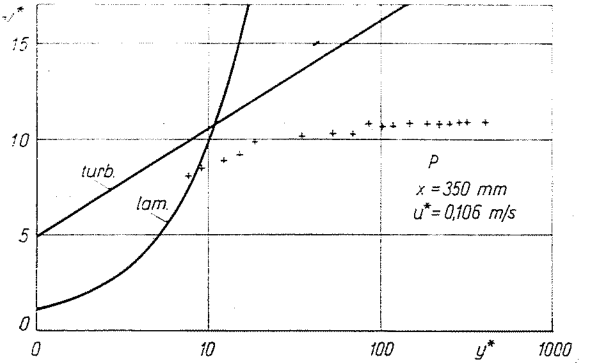

Fig. 7c

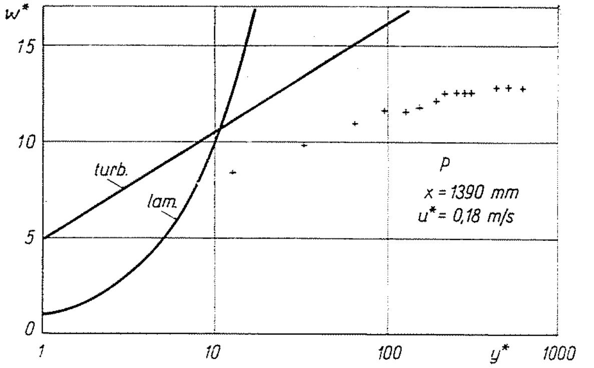

Fig. 7d

The relatively long logarithmic portions of the curves are well recognized, the superimposed velocity distributions described by the "law of the wake" [2], the so-called Coles profiles are relatively small.

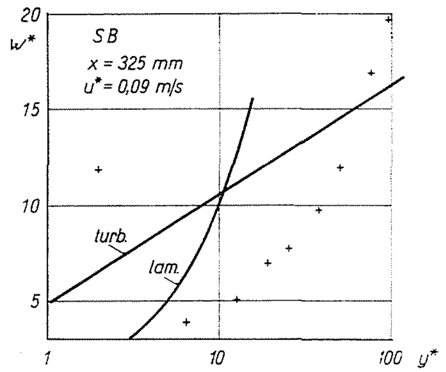

Fig. 7e

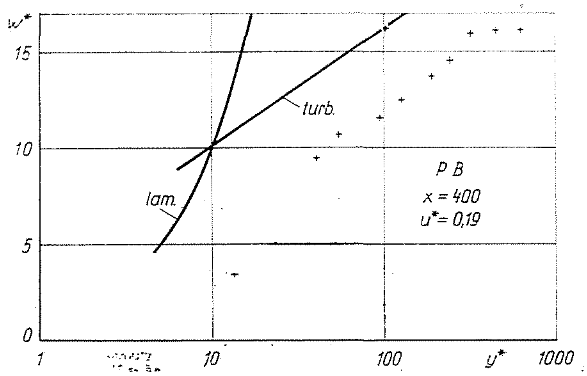

Fig. 7f

Fig. 7e and 7f show profiles taken in the presence of the streamline body (B in Fig. 3) for x values measured from the point 0' and indicated in the figures. In these cases the Coles profiles play a predominant role.

Throughout Fig. 7a—f the relationship (2) valid in the laminar sublayer, and the relation

$$w^* = S \log y^* + B \tag{5}$$

valid for the turbulent part of the layer in absence of rotation [4] are represented, the numerical values being $S = 5.66$ and $B = 4.9$, respectively.

It can be seen from the Fig. 7a—d, that in our cases the slope of the logarithmic profile departs from the slope valid in stationary boundary layers. On the suction side the slopes are higher, on the pressure side lower than in the non-rotating case.

The data of the other profiles not detailed here corroborate the above statement. Thus the formula

$$w^* = S_\omega \log y^* + B_\omega \tag{6}$$

describes the "law of the wall" in rotating systems as well, the quantities S_ω and B_ω, however, differ from the constants S and B determined in the stationary case. In order to enlighten the problem the slopes of 10 profiles evaluated are plotted in Fig. 8 as a function of the quantity

$$\Omega = 2\,\omega u^{*2} \left[\frac{\mathrm{m}^2}{\mathrm{s}^3}\right] \tag{7}$$

justified later.

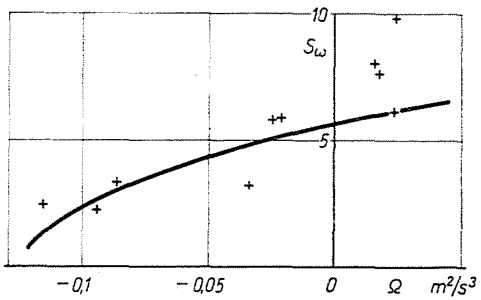

Fig. 8. The relation $S_\omega(\Omega)$

In spite of the considerable experimental scatter the trend is clearly seen: for positive values of Ω, which, according to the following, correspond to the suction side, S_ω is greater whereas on the pressure side S_ω is smaller than S.

Similarly a departure can be observed in connection with B_ω, the scatter, however, does not allow any reliable numerical evaluation.

4. Theoretical considerations

The above results support a hypothesis originating from GRUBER [3] on the influence of the Coriolis forces caused by the fact of rotation, which stabilize the turbulent fluctuations on the suction side and create instability on the pressure side. The hypothesis will be enlightened on the basis of the Fig. 9, where the distribution of the relative velocity at the suction side and pressure side of a blade are shown. Representing the Coriolis forces

$$\mathbf{a}_c = 2\,\mathbf{w} \times \omega \tag{8}$$

the instable character of the field at the side P, and stable character at the side S can be seen. Let us assume that in the case represented in Fig. 9 the effect of the Coriolis forces is proportional to the quantity

$$\operatorname{div} \mathbf{a}_c = 2\,\omega \operatorname{rot} \mathbf{w} - \mathbf{w} \operatorname{rot} \omega\,. \tag{9}$$

The angular velocity ω in the rotating system being constant, it follows according to Fig. 9, that

$$|\operatorname{div} a_c| = |2\,\omega \operatorname{rot} w| = \pm\, 2\,\omega \frac{\partial w}{\partial y} \tag{10}$$

where positive and negative sign correspond to the suction and the pressure sides, respectively.

For sake of simplicity, regarding the turbulent flow in the boundary layer as a damped, forced vibrating system, it may be assumed that the

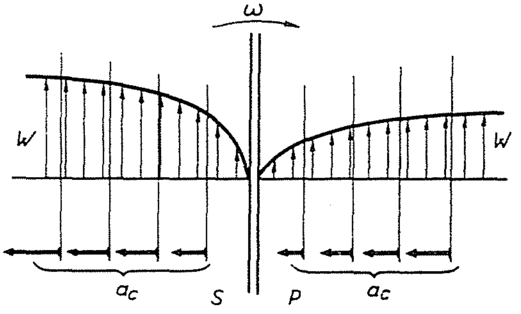

Fig. 9. Coriolis forces in the boundary layer

system is in the state of resonance, since the fluid particles force each other with the frequency of their own motion.

The damping effect of the Coriolis forces may be regarded as a change in the spring constant of the system. Since the spring constant of the Coriolis forces regarding the dimensions is

$$C_c = \frac{1}{m\,|\operatorname{div} a_c|} = \frac{1}{m\left|\,2\,\omega \dfrac{\partial w}{\partial y}\right|}, \tag{11}$$

where m is the mass of the turbulent vibrating system, the resultant spring constant C_ω of the system with the original spring constant C (in the stationary case) can be calculated from

$$\frac{1}{C_\omega} = \frac{1}{C} + \frac{1}{C_c} = \frac{1 + Cm\,2\omega \cdot \partial w/\partial y}{C}\,. \tag{12}$$

The amplitude of the vibration, which can be taken as proportional to the mixing length l [4] applied in the theory of turbulent flows, changes according to

$$\left(\frac{l_\omega}{l}\right)^2 = \frac{C_\omega}{C} = \frac{1}{1 + mC\,2\omega \cdot \partial w/\partial y}\,; \tag{13}$$

the other circumstances supposed to be the same.

The introduction of the frequency α defined by

$$mC = \frac{1}{\alpha^2} \tag{14}$$

gives

$$\left(\frac{l_\omega}{l}\right)^2 = \frac{1}{1 + \frac{2\omega\, \partial w/\partial y}{\alpha^2}} \,. \tag{15}$$

As it is known [4] the mixing length may be expressed by the aid of a universal constant:

$$l = \varkappa y \,. \tag{16}$$

Similarly, by introducing the constant $\varkappa_\omega$ defined by the equation

$$l_\omega = \varkappa_\omega y \tag{17}$$

for the case of rotation, on the basis of (15) it follows:

$$\varkappa_\omega = \frac{\varkappa}{\sqrt{1 + \frac{2\,\omega\, \partial w/\partial y}{\alpha^2}}} \,, \tag{18}$$

Thus $\varkappa_\omega$ is no more universal, it depends among others on ω. The expression in the denominator of (18) may now be transformed:

$$\frac{\partial w}{\partial y} = \frac{u^{*2}}{\nu} \; \frac{dw/u^*}{dyu^*/\nu} = \frac{u^{*2}}{\nu y^*} \; \frac{dw^*}{d\ln y^*} \,, \tag{19}$$

so, with the abbreviation

$$a = \frac{1}{\alpha^2 \nu y^*} \cdot \frac{dw^*}{d\ln y^*} \tag{20}$$

on the basis of (7) equation (18) changes to

$$\varkappa_\omega = \frac{\varkappa}{\sqrt{1 + a\Omega}} \,. \tag{21}$$

As a first rough approximation it is supposed that the value in (20) may be substituted by a mean value nearly constant in all cases.

As [4]

$$S = \frac{2{,}303}{\varkappa}, \tag{22}$$

with

$$S_\omega = \frac{2{,}303}{\varkappa_\omega} \tag{23}$$

we get

$$S_\omega = S\sqrt{1 + a\Omega} \tag{24}$$

which is an approximate formula for the slope of the logarithmic velocity profile on the impeller blading.

The concrete form of equation (24) calculated with $a = 8$ s^3/m^2 is represented in Fig. 8.

The deviations from the measured values arise partly from substituting equation (20) by a constant, partly from the experimental error, and partly from the simplicity of the theory: their separation is difficult.

Symbols

a	abbreviation, *(20)*
$\mathbf{a}_c$	Coriolis field strength
B	numerical constant, *(5)*
C	spring constant
C_c	spring constant, *(11)*
l	mixing length
m	mass
n	revolutions per minute
Re	Reynolds number
S	slope of the logarithmic profile
u^*	frictional velocity, *(1)*
w, $\mathbf{w}$	relative velocity
$w^* = w/u^*$	*(3)*
$y^* = yu^*/\nu$	*(4)*
$\varkappa$	universal constant, *(16)*
ν	kinematic viscosity
ϱ	density
τ	wall shear stress
ω, $\boldsymbol{\omega}$	angular velocity of the impelles
Ω	abbreviation, *(7)*

Indices

ω	quantities interpreted in rotating systems

Summary

The experimental results clearly indicate that in turbulent boundary layers on the blading of radial impellers both the logarithmic and Coles-profiles are valid.

Owing to the influence of the Coriolis forces the slope of the logarithmic profile departs from the value found for stationary cases. The reasons of this departure may be given by a simplified theory.

The change in form of the Coles-profile caused by the Coriolis-forces cannot be indicated unambigously at present because of the experimental scatter.

The paper omits the discussion of the functional relations and their variation caused by the rotation which describe the streamwise change of the velocity profiles.

The solution of these problems needs further, extended investigations.

References

1. LITVAI, E.: Investigation of the boundary layer on radial impellers. Scient. Session 1967, of the Techn. Univ. Budapest. 1, 179—193. Budapest, 1967. (in Hungarian). See also: Comment on Prof. Kline's paper in: Brown Bovery Symposium "Flow Research on Blading" 1969. To be published by Elsevier Publishing Co., Amsterdam.
2. COLES, D.: The law of the wake in the turbulent boundary layer. J. Fluid Mech. 1, 191 (1956).
3. GRUBER, J. — LITVAI, E.: An investigation of the effects caused by fluid friction in radial impellers. Proc. 3. Conf. Fluid Mech. Budapest. 1969. 241—247.
4. SCHLICHTING, H.: Grenzschicht-Theorie. Karlsruhe, 1965.

Dr. Elemér LITVAI
Dr. László PRESZLER
Budapest, XI., Bertalan Lajos u. 4—6. Hungary